Progress In Electromagnetics Research C, Vol. 89, 221–231, 2019

A CPW-Fed CSRR and Inverted U Slot Loaded Triple Band Notched UWB Antenna

Ajay Yadav[1, 2, *], Mamta D. Sharma[1], and Rajendra P. Yadav[2]

Abstract—A CPW-fed ultra-wideband (UWB) monopole antenna design which exhibits triple band stop functions is demonstrated. The proposed antenna comprises a Split Ring Resonator (SRR) and inverted U slots on a metallic patch to exhibit triple band-notch functions for WiMAX (3.3–3.6 GHz), C-band (3.8–4.2 GHz) and WLAN (5.1–5.8 GHz) bands. The slot width optimization is examined to tune the band-notch resonance frequency, and their effects are exhibited by surface current distributions. The antenna has compact size of $26 * 30\,\text{mm}^2$, and it functions over 3 to 11 GHz with VSWR < 2 except notched bands. The SRR loaded dual band-notched antenna and amended inverted U slot integrated antenna both are fabricated and their VSWR, radiation characteristics measured. The antenna demonstrates excellent agreement between measured and calculated results.

1. INTRODUCTION

The present wireless communication development has a great demand of antennas with large bandwidth. Particularly for short range communications, large bandwidth antennas are highly desirable to communicate at high data rate and overcome the limitations of narrow band antennas. However, these large bandwidth antennas accommodate narrowband applications too [1]. Large bandwidth antennas are highly appreciated for UWB technology to fulfill the requirement of high data rate and overcome other limitations like data encryption, minimum possibility of data interception and many more [2]. On February 14, 2002, an unlicensed band called UWB from 3.1 to 10.6 GHz with a span of 7.5 GHz was declared by the Federal Communication Commission (FCC) for commercial applications [3]. Microstrip or planar antennas are highly recommended for UWB technology because of their undisputed advantages over other antennas and so forth [4].

A UWB technology device suffers from problems like electromagnetic interventions caused by other existing narrow band spectra for communications such as WiMAX, WLAN systems, C and X-band satellite communication (3.8–4.2 GHz and 7.25-8.4 GHz respectively).

In the last few years, to resolve the EM intervention complication, researchers have presented diverse approaches. To develop antennas with band filtering features, recently few methods have been reported namely, an L slot in the ground plane [5], an inverted U slot on a radiating structure [6], a C-shape slot on a metallic patch [7], simple vertical and horizontal rectangular slots etched on metallic patch for band stop feature at high frequencies [8], W and C slots [9], an SRR slot on a radiating patch and N shape feed line miniature [10], elliptical and rectangular CSRRs to create triple band notches [11], arc shape and elliptical SRR [12], rectangular SRR near feed line [13], meander shape stub, rectangular SRR and inverted U slot with L shape parasitic stubs at ground plane [14] and CSRR, S shape feed line miniature and circular SRR near feed line [15, 16].

Received 21 October 2018, Accepted 18 December 2018, Scheduled 7 January 2019
* Corresponding author: Ajay Yadav (ajay.yadav.1981@ieee.org).
[1] Department of ECE, Global Institute of Technology, Jaipur, India. [2] Department of ECE, Malaviya National Institute of Technology, Jaipur, India.

In the proposed antenna, we have put forward nested rectangular SRR etched on a radiating structure to produce dual band-stop features in WiMAX, WLAN band and an inverted U-slot to produce C-band notched feature. The frequency span between WiMAX and C-band notches is quite small (200 MHz), but this unlicensed band can be used for short range communications without any interfering signals. However here we analyze the much closed band notched characteristics without affecting the other unlicensed frequency spectrum. In this paper, analysis of the parametric deviations has been implemented for all the slots and their coupling effects presented through current distribution. As mentioned above, many researchers have exhibited distinct methods to produce band notching characteristics in UWB antennas, but all these methods have been exercised on slot length or parasitic element length in terms of wavelength to tune the band notch frequency while they have failed to examine the slot width or parasitic element width for the tuning of band-notched resonance frequency. Here we have observed the slot width parametric variations to tune the band-notched resonance frequency. By the parametric variation of slot width, we have realized that slot width is also an alternative to tune the band notch resonance frequency keeping slot length constant for desired band notch resonance frequency. The concept behind the slot width variation is its effects on effective capacitance. The effective capacitance increases/decreases with narrowing/widening the slot width which produces lower/higher resonance frequency for band notch. Another benefit of implementing this innovative idea is to overcome the RF leakage from radiating patch. The presented antenna developed on the primary antenna is used in [8] whereas SRR dimensions and their position have also been modified as the antenna in [17]. For better understanding the fabricated antenna and its measured and simulated results are presented here with detailed explanation.

2. DESIGN AND SIMULATED RESULTS ANALYSIS

The presented antenna designs have been prepared with commercially available electromagnetic simulator Ansoft's HFSS. The suggested design is constructed on FR-4 material with a depth of 1.6 mm, permittivity $\varepsilon_r = 4.4$ and loss tangent of 0.02. The step by step evolution of designed antenna is presented in Fig. 1. Fig. 1 depicts the UWB primary antenna which covers the complete UWB (3.1–

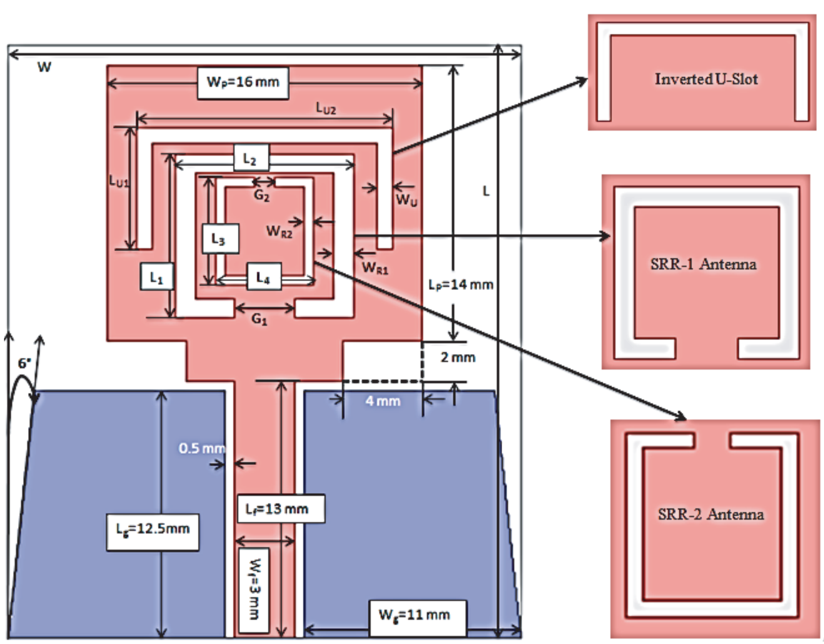

Figure 1. Proposed triple band notched UWB antenna integrated with inverted U-slot antenna, SRR-1 antenna and SRR-2 antenna. $W = 26\,\text{mm}$, $L = 30\,\text{mm}$, $L_{U1} = 6.1\,\text{mm}$, $L_{U2} = 13\,\text{mm}$, $L_1 = 8.3\,\text{mm}$, $L_2 = 9\,\text{mm}$, $G_1 = 3\,\text{mm}$, $W_{R1} = 1\,\text{mm}$, $W_U = 0.8\,\text{mm}$, $L_3 = 5.38\,\text{mm}$, $L_4 = 4\,\text{mm}$, $W_{R2} = 0.48\,\text{mm}$ and $G_2 = 1\,\text{mm}$.

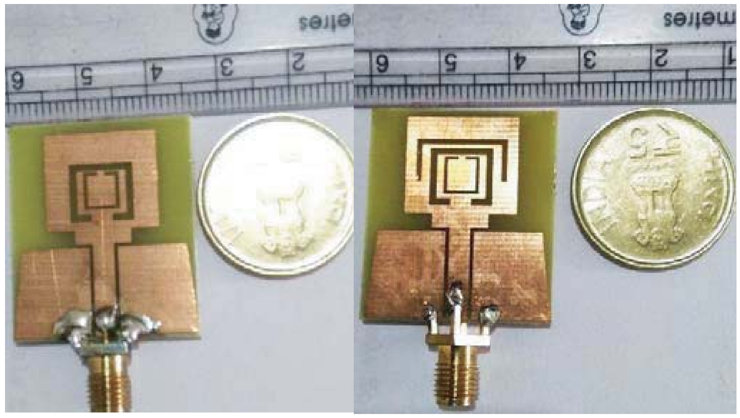

(a) (b)

Figure 2. Proposed triple band stop antenna geometry. (a) Dual band notched UWB antenna. (b) Proposed band notched UWB antenna.

106 GHz) spectrum. Primary antenna is integrated with WiMAX band-notched SRR-1 slot, WLAN band-notched SRR-2 slot and inverted U slot to produce C-band notched function. To provide matching with port impedance 50 Ω a feedline width of 2.8 mm was chosen. We have preferred primary antenna as in [8] that covers complete UWB spectrum and revised the dimensions for optimum performance of the antenna presented in [17]. Further, a prototype is manufactured and measured to validate the band notching characteristics for WiMAX and WLAN applications. A triple band notched antenna incorporates an inverted U slot on modified antenna and is shown in Fig. 2. During the optimization of both the antennas, precautions have been taken to minimize their coupling effects on other slots, and it can be verified from the current distribution presented in Fig. 9. The evolution of suggested antenna has been described through three steps and discussed in this section.

2.1. Step-1 (Primary Antenna with SRR-1 Slot)

To achieve band stop performance at WiMAX band, SRR-1 slot has been etched on a metallic patch. The total slot length is closely equivalent to $\lambda g/2$. The length of SRR-1 slot can be planned with Equations (1) and (2).

$$L_{eq} = \{2 * (L_m + L_n) - G_x - 4W_{Rx}\} \quad (1)$$

$$f_r = \frac{C}{2 * L_{eq} * \sqrt{\frac{\varepsilon_r + 1}{2}}} \quad (2)$$

where

f_r = Resonance frequency of notched band
L_{eq} = Equivalent length of SRR-1 slot
ε_r = Relative permittivity of substrate
c = Speed of light (3×10^8 m/s)

Suffixes m and n show the SRR side lengths, and x shows the respective SRR number. For SRR-1 in Equation (1) $m = 1$ and $n = 2$ whereas for SRR-2 slot $m = 3$ and $n = 4$.

The slot equivalent length L_{eq} can be operated with the changes in gap "G_1", here an optimized one is 3 mm. It can be adjusted to produce a band stop performance at WiMAX band. The calculated slot length to produce band notch is 25.66 mm whereas the optimized length is 27.6 mm. Slot width plays a significant role to tune the desired resonance frequency of band notch and is discussed in Fig. 7.

2.2. Step-2 (Primary Antenna with SRR-2 Slot)

We have proposed an SRR-2 slot loaded antenna to produce band stop function for frequency band lying between 5.1 and 5.8 GHz (WLAN) applications. The effective equivalent length of designed SRR-2 can be evaluated from Equation (1) and Equation (2). The calculated equivalent length of the SRR-2 to generate band notch at WLAN band is 15.84 mm whereas the optimized slot length is 17.84 mm.

2.3. Step-3 (Primary Antenna with Inverted U-Slot)

An inverted U shape etched antenna is employed to produce band-notched function for the center frequency of C-band (3.8 to 4.2 GHz) at 4 GHz resonant frequency, and its preliminary length can be evaluated using Equations (3) and (2). The calculated slot length of the inverted U slot is 22.86 mm, and optimized slot length is 22.8 mm. The slot length is varied (specially L_{U1}) by keeping width W_U fixed at 0.8 mm to resonate it at 4 GHz.

$$L_{Ueq} = \{(2 * L_{U1}) + L_{U2}\} - (3 * W_U) \tag{3}$$

The desired triple band stop feature has been attained by integrating all the explained steps.

The basic UWB antenna (a square shape metallic patch) furnishes a VSWR less than 2 as displayed in Fig. 3. The proposed antenna and its evolution stages as band notching characteristics in terms of VSWR results are encapsulated in Fig. 3, and the recommended one is represented by a hard line.

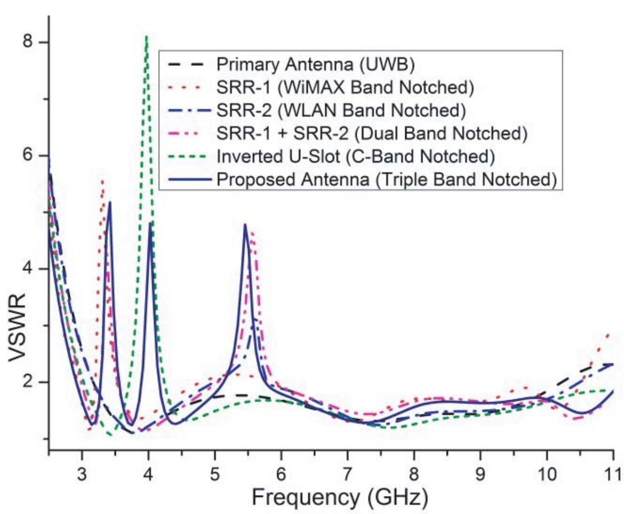

Figure 3. VSWR vs frequency (step by step evolution of proposed design).

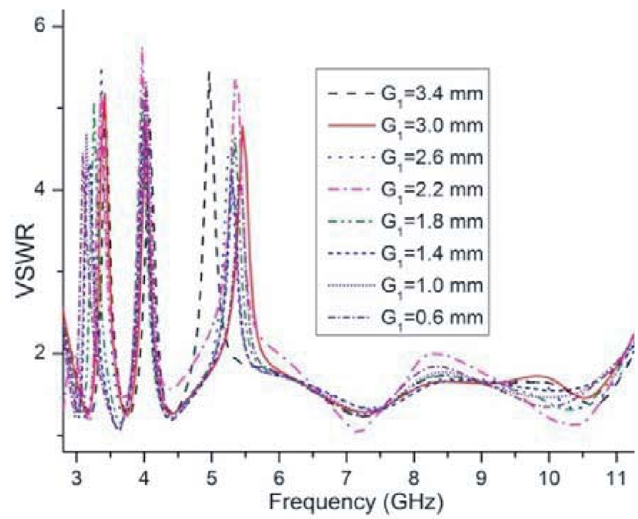

Figure 4. Effects of variations in gap G_1 on VSWR.

An optimized length L_{eq} of slot SRR-1 can be computed through Equation (1). The gap size G_{R1} can be used to optimize SRR-1 slot dimensions. The distinct VSWR results have been received with varying gap dimensions and presented in Fig. 4. The slot resonance frequency of band notch is inversely proportional to the effective inductance due to the slot length. Here we have kept slot width constant at 1 mm. From Fig. 4 it is clearly visualized that the proximity between SRR-1 and SRR-2 slots generates an extra effective capacitance and causes the shift in resonance frequency of WLAN band with changes in SRR-1 slot length. The aforesaid concept can be verified from the current distribution as shown in Fig. 9(a).

The SRR-2 slot length L_{Ueq} can be optimized with Equation (1) and gap G_2. We have kept slot width constant at 0.48 mm and altered gap dimension G_2 to optimize the SRR-2 slot length, and VSWR results are presented in Fig. 5. The length of SRR-2 decreases with increment in G_2, and resonance frequency of notch band is shifted towards a higher frequency. In Fig. 5 one can see that there is negligible effect of SRR-2 slot length, and the same result is derived in Fig. 9(c) which depicts the current distribution of proposed antenna.

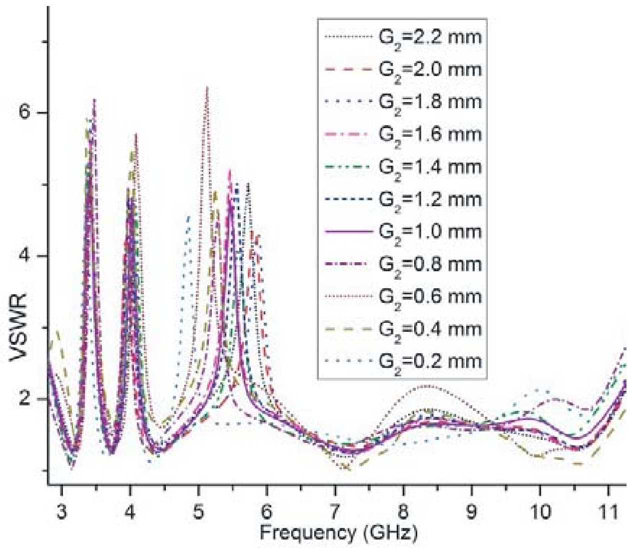

Figure 5. SRR-2 gap G_2 length alteration and VSWR results.

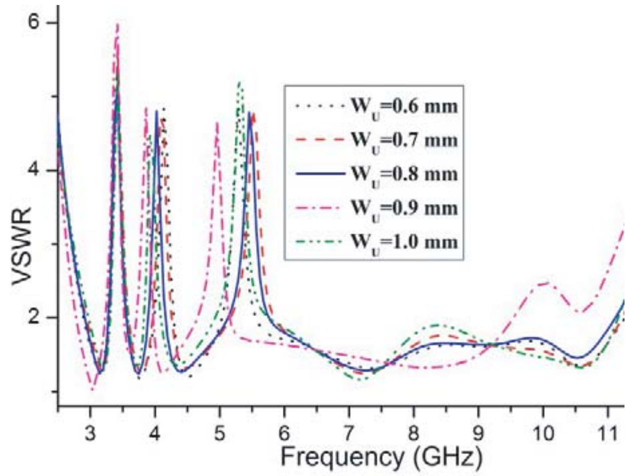

Figure 6. Inverted U slot width variation and VSWR.

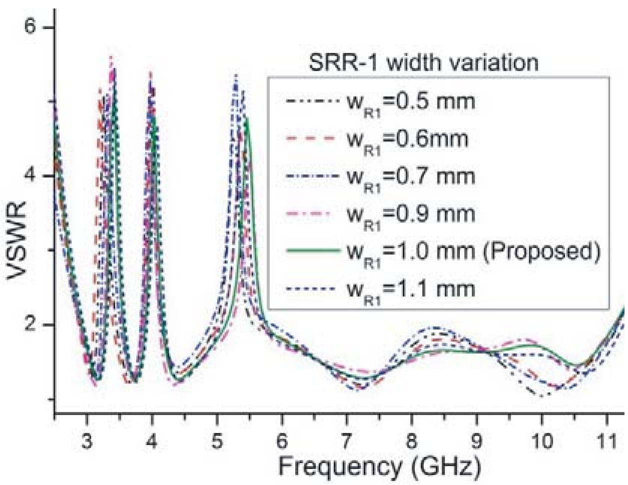

Figure 7. SRR-1 slot width and VSWR.

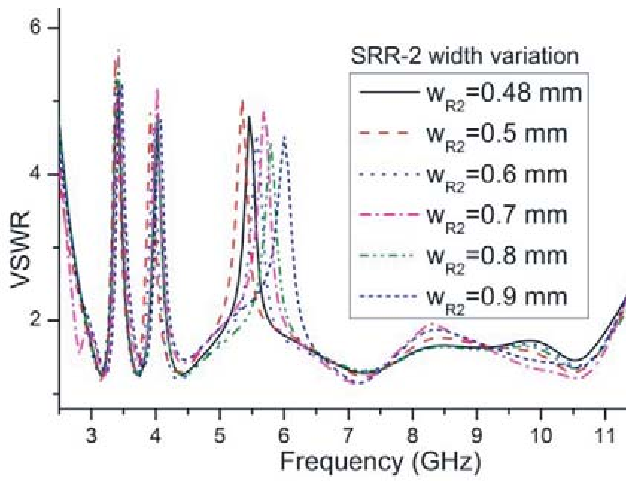

Figure 8. SRR-2 slot width and VSWR.

Figure 6 shows the width optimization of the inverted U slot, and it is evident that the resonance frequency of the band notch can be tuned with variation in slot width. The result can be verified by Equation (3). The effective capacitance also affects other slot characteristics to produce resonance frequency of band notch.

In Fig. 7, the variation in width of SRR-1 produces the same variation as shown in Fig. 4. The width of SRR-1 also affects the SRR-2 slot resonance frequency of band notch due to the effective capacitance.

In Fig. 6, the effects of inverted U-slot on the VSWR of the triple notched band antenna are presented. It is evident that tuning the resonance frequency of band notch through variation in slot width can be compared with the results in Fig. 5. Tuning of slot width produces a more accurate result than tuning the length of the slot, and it can be verified from the measured result in Figs. 11 & 12, respectively.

The consequence of current distribution on the suggested antenna at various frequencies is depicted in Fig. 9. At chosen frequencies like 3.45, 4 & 5.5 GHz which are the stopbands, an inconsistent current

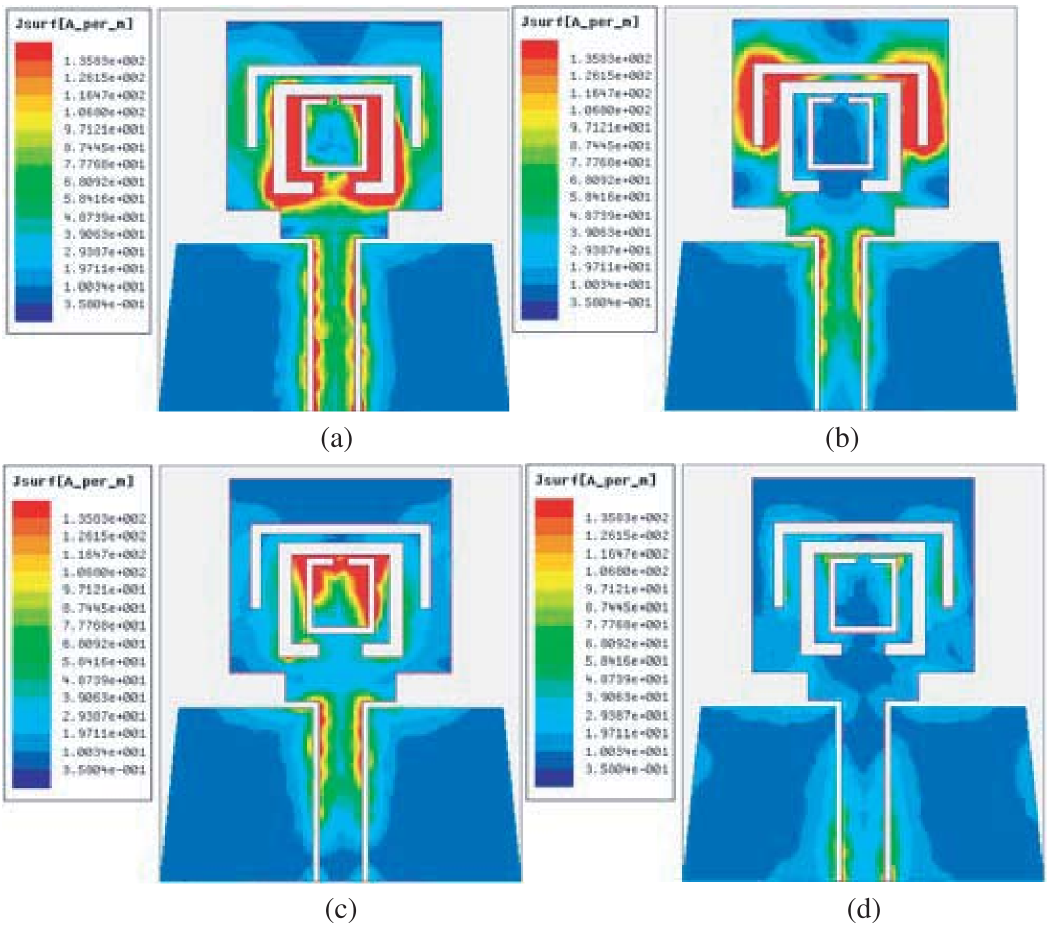

Figure 9. Current distribution at distinct frequencies. (a) 3.45 GHz, (b) 4 GHz, (c) 5.5 GHz, (d) 4.6 GHz.

accumulation is found near edges of the corresponding slot whereas uniform current distribution for passband (4.6 GHz) as displayed in Figs. 9(a)–(d). The nonuniform current accumulation at center resonance frequency of WiMAX band notch is depicted in Fig. 9(a). A nonuniform current accumulation produces impedance difference which bears positive sign to generate band notch phenomenon at the desired frequency. However, the maximum current accumulation results in generation of an effective inductance, and width of the slot represents effective capacitance. The effective inductance and capacitance can affect the other slot characteristics. It can be seen from Fig. 9(a) that at 3.45 GHz there is an accumulation of current around SRR-1 as well as around SRR-2 slot which changes the effective inductance and capacitance of the SRR-2 slot, and it is evident in Fig. 4 and Fig. 7. In Fig. 9(b), the current scattering at 4 GHz is presented, and maximum current accumulation is around the inverted U slot open ends whereas minimum current is at the upper part of the slot, and it is an evidence of impedance difference and causes the band notch at the desired frequency. It can be observed in Fig. 9(b) that at 4 GHz current accumulation around SRR-1 and SRR-2 slot is found which changes the effective capacitance. Due to changes in the effective capacitance (effective capacitance of SRR-1 is more than SRR-2 due to more current accumulation), the resonance frequency of band notch shifts according to the loose or strong coupling capacitance as represented in Fig. 6. Likewise, Fig. 9(c) depicts the current distribution at 5.5 GHz, and maximum current accumulation is found near the open end of the SRR-2 slot which proves the band notch creation at the desired frequency. For the passband or the frequency where the antenna is radiating or receiving the power, the current distribution is uniform, and it can be verified from Fig. 9(d) which shows the current distribution at 4.6 GHz.

Figure 10 demonstrates input impedance characteristics of the recommended antenna with

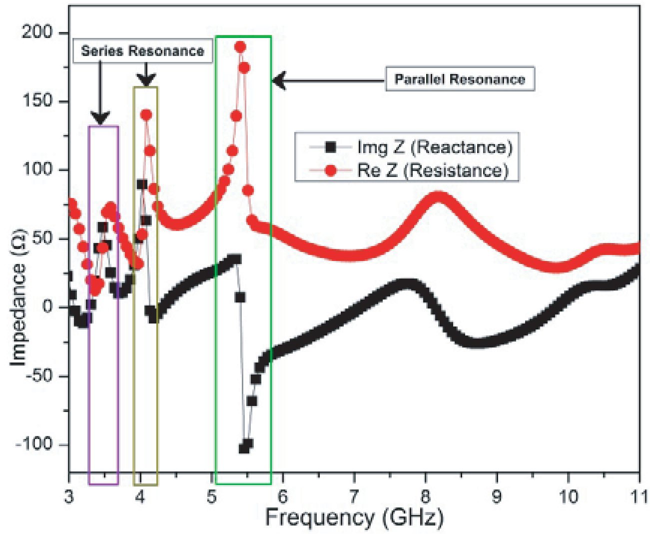

Figure 10. Input impedance of designed antenna.

frequency. The introduced antenna shows resistance approximately equal to 50 Ω for resonating frequencies and approximately zero for reactances. At band-notched frequencies it can be seen that these values are not uniform. At band-notched frequencies 3.5 and 4 GHz, it can be observed that resistance varies from 75 to approximately 140 Ω whereas reactances at both the frequencies have positive derivative which indicates a series type resonance to generate band notch function. Likewise, at 5.5 GHz, it can be observed that the input resistance has a very high value approximately 200 Ω, and input reactance is a negative derivative which produces a parallel resonance and an evidence to produce band-stop functions at the desired resonance frequency of band notch.

3. MEASURED RESULTS OF PROPOSED ANTENNA

The discrepancies between EM simulator generated and measured outcomes of dual band and triple band notched antennas are presented in Fig. 11 and Fig. 12, respectively. The primary antenna integrated with SRR-1, SRR-2 and inverted U slots are positively producing dual notched band for WiMAX, WLAN and C-band along with keeping UWB working from 3.1 to 11 GHz with satisfactory VSWR. The radiation performances at distinct frequencies like 3.75, 4.5 and 7.5 GHz are represented in Figs. 13(a), (b) & (C).

The suggested triple band-notched antenna exhibits excellent agreement between calculated and measured VSWRs. Fig. 12 shows that the proposed triple band-notched antenna has excellent agreement

Table 1. Comparison of various parameters for individual notch band.

Characteristics ↓ **Band Notches** →	**WiMAX**	**C-Band**	**WLAN**
Theoretical BW (GHz)	3.3–3.6	3.8–4.2	5.1–5.8
Designed Notch Frequency (GHz)	3.5	4	5.5
Simulated Notch Frequency (GHz)	3.42	4	5.45
Simulated BW (GHz)	3.27–3.59	3.82–4.19	5.12–5.79
Calculated Slot Length (mm)	26.13	22.86	16.63
Optimized Slot Length (mm)	27.6	22.8	17.84
% Error between Calculated and Optimized Length	5	0.2	7

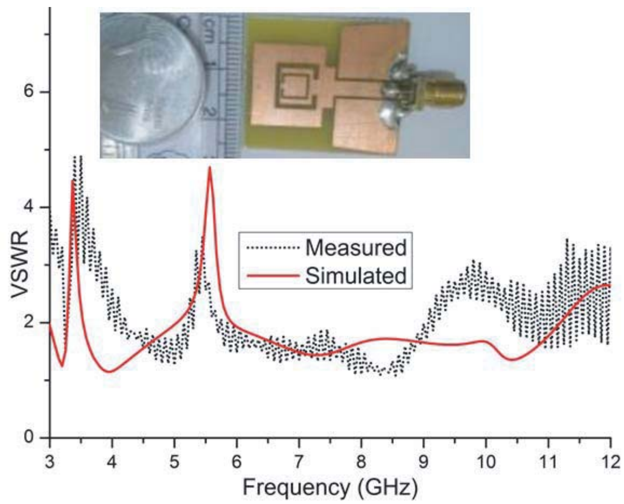

Figure 11. VSWR of dual band antenna.

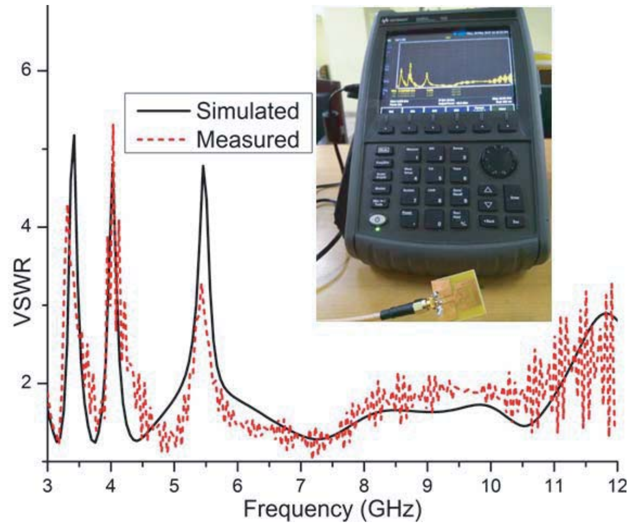

Figure 12. VSWR of triple band antenna.

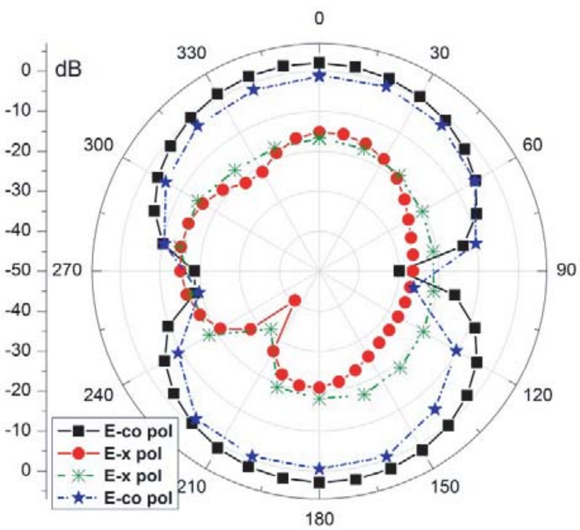

(a)

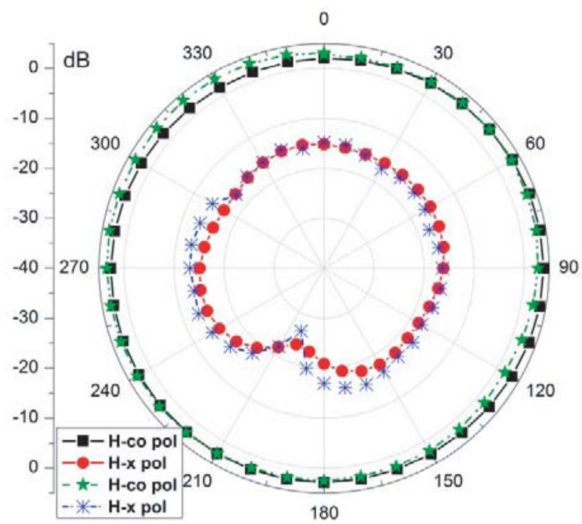

(b)

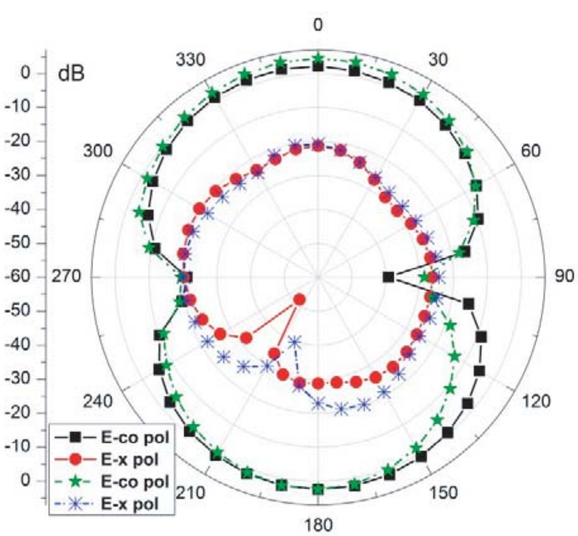

(c)

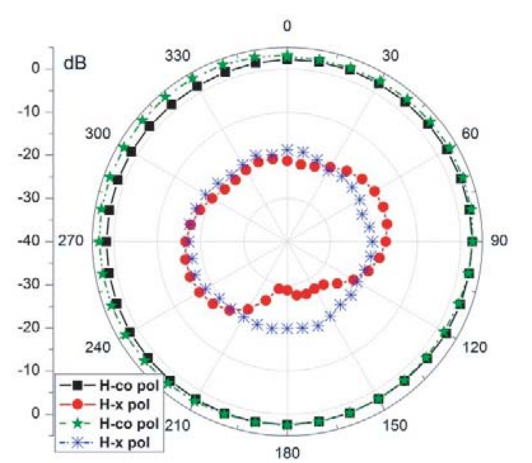

(d)

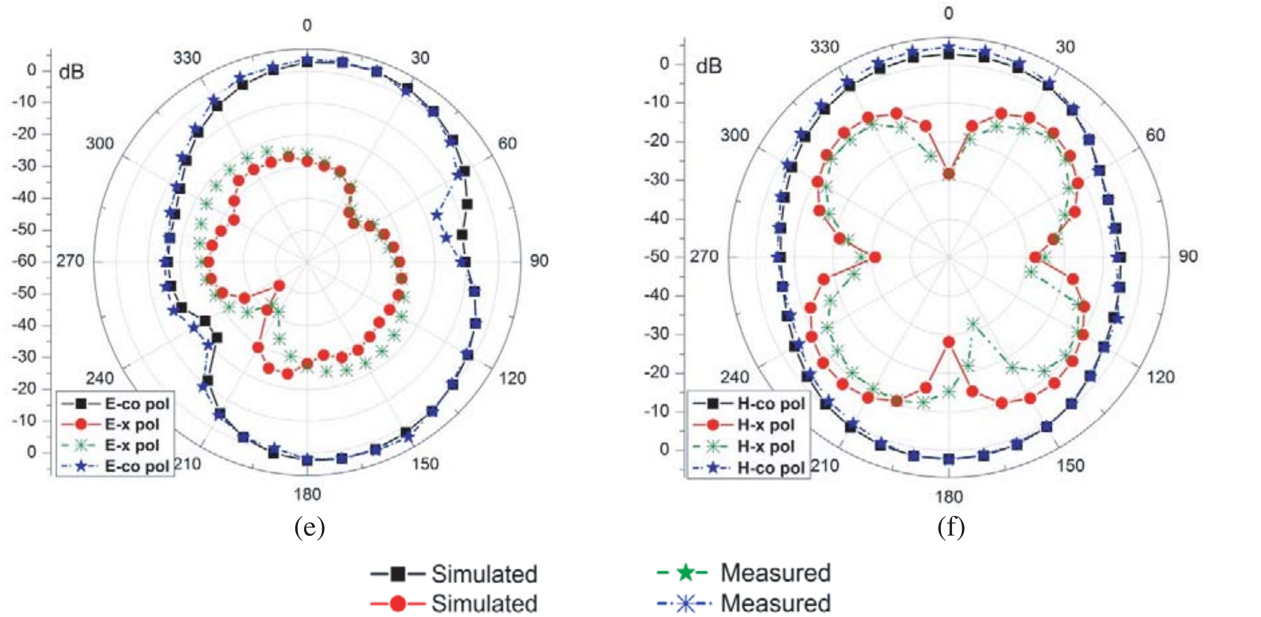

Figure 13. Simulated and measured E-field (XZ plane) and H-field (YZ plane). (a) 3.75 GHz (E-field), (b) 3.75 GHz (H-field), (c) 4.5 GHz (E-field), (d) 4.5 GHz (H-field), (e) 7.5 GHz (E-field), (f) 7.5 GHz (H-field).

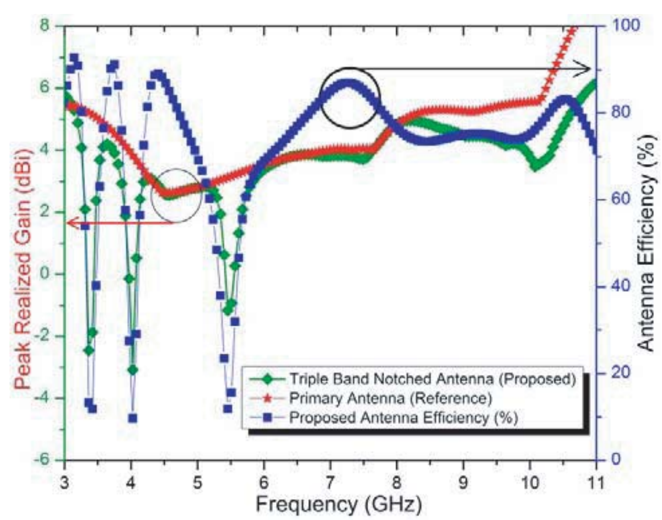

Figure 14. Peak realized gain and antenna efficiency vs frequency.

between measured and simulated results which also verifies the proposed band notching methods. The radiation characteristic of the suggested antenna has been measured in an anechoic chamber for co & cross polarizations, and results are presented for various frequencies in Fig. 13. The proposed antenna has good agreement between simulated and measured radiation characteristics in both the planes namely XZ (E-field) and YZ (H-field). The proposed antenna radiation pattern shows identical pattern to dipole antenna in E-field (XZ plane) and omnidirectional pattern in H-field (YZ plane) which is essential for a UWB antenna. Radiation characteristics at high frequencies deviate from the omnidirectional pattern in E-field due to the appearance of higher order modes.

Some useful information of presented work and used references is listed in Table 1.

Figure 14 shows the antenna efficiency and gain with frequency. It can be observed that antenna efficiency for the band-notched frequencies like 3.5 GHz, 4 GHz and 5.5 GHz is very low and approximately 10% which is the evidence that the proposed antenna cannot radiate or receive EM power at these frequencies, whereas for the passband frequencies it shows an average efficiency of 80%. It can also be observed that at notched-band frequencies the gain of proposed antenna is negative, which is again an evidence that at notched frequencies antenna radiates or receives negligible power, whereas for passbands it has a uniform gain approximately 4 to 5 dBi. The band notching structures etched on primary antenna are the main cause (power leakage during resonance) which decreases the gain of proposed antenna in comparison to primary antenna, and it can be seen from Fig. 14. Some useful information about the presented antenna with respect to recently presented antenna is listed in Table 2.

Table 2. Comparison of proposed antenna with recently presented antennas.

Ref. []	Size (mm^3)	ε_r	No. of Notch	Band Notch Gain (dBi)	Frequency Band (GHz)
[6]	$24 \times 26 \times 1.6$	4.2	1 (WLAN)	−1.58	3–12
[7]	$31 \times 40 \times 0.635$	10.2	1 (WLAN)	NA	3–10.28
[8]	$26 \times 30 \times 1.6$	4.4	2 (WLAN, X-Band)	0, −16	3.1–10.6
[9]	$37 \times 40 \times 1.6$	4.4	2 (WiMAX, WLAN)	−7, −6	2.5–11.5
[10]	$30 \times 40 \times 1$	4.5	2 (WiMAX, WLAN)	−11, −9	2.0–10.6
[11]	$35 \times 35 \times 1.6$	4.4	3 (WiMAX, WLAN, X-Band)	−5, −1, −3	2.21–12.83
[12]	$30 \times 35\,mm^2$	NA	3 (WiMAX, WLAN, X-Band)	−2, −2, −3	2.8–11.42
[13]	$40 \times 40 \times 0.812$	3.38	3 (WiMAX, WLAN, ITU Band)	NA	3–11
[14]	$30 \times 30 \times 1.6$	4.4	3 (WiMAX, WLAN, ITU Band)	1, 1.5, 1	3–12
[15]	$26 \times 30 \times 1.6$	4.4	3 (WiMAX, WLAN, X-Band)	−5, −5, −0.5	3–11
[16]	$26 \times 30 \times 1.6$	4.4	2 (WiMAX, WLAN)	−7, −4	3–11
Present Work	$26 \times 30 \times 1.6$	4.4	3 (WiMAX, C-Band, WLAN)	−2.8, −3.5, −1.5	3–11

4. CONCLUSIONS

A CPW-fed planar antenna with triple band-stop characteristic is designed to reduce prospective EM interventions due to narrowband uses. Incorporating all band-notched elements namely SRR-1, SRR-2 and inverted U slot utmost care has been taken to minimize their cross-coupling effect. The recommended antenna operates over 3 to 11 GHz which includes the UWB spectrum for low power applications. This antenna successfully exhibites triple band-notched characteristics and shows excellent agreement between simulated and measured results. We have studied the slot width variation and found that it is a good alternative to tune the resonance frequency of band notch, and the same is reflected in various figures plotted. The suggested antenna has a very compact size of $26 \times 30\,mm^2$ with triple band notched at WiMAX, C-band, and WLAN which make it a suitable candidate for band-notched applications, short-range communications with improved interferences performance and applications where small size is the figure of merit. The proposed antenna has very low efficiency (10%) for band-notched frequencies and negative gain whereas 80% efficiency and gain vary from 4 to 5 dBi for passband frequencies. Furthermore, the designed antenna may be improved in mathematical equations for tuning the resonance frequency with slot width.

ACKNOWLEDGMENT

We are thankful to Prof. Kumar Vaibhav Srivastava of Indian Institute of Technology, Kanpur, India for providing the measuring facility for radiation pattern measurement in RF microwave lab and an anechoic chamber. We also admire the Vice-Chairman and Director of Global Institute of Technology, Jaipur, India for providing VNA for the measurement in Center For Excellence.

REFERENCES

1. Chen, Z. N. and M. Y. W. Chia, *Broadband Planar Antennas: Design and Applications*, John Wiley & Sons, Chichester, UK, 2006.
2. Ray, K. P., "Design aspects of printed monopole antenna for ultra-wideband applications," *Int. J. Antennas Propag.*, 1–8, 2008, http://dx.doi.org/10.1155/2008/71385.
3. First Report and Order, "Revision of Part 15 of the Commission's rule regarding ultra-wideband transmission system," Federal Communications Commission, FCC 02-48, 2002.
4. Chen, Z. N., "UWB antennas: From hype, promise to reality," *IEEE Antennas Propag. Conf.*, 19–22, 2007.
5. Shambavi, K. and C. A. Zachariah, "Printed dipole antenna with band rejection characteristics for UWB application," *IEEE Antennas Wirel. Propag. Lett.*, Vol. 9, 1029–1032, 2010.
6. Seo, Y. S., J. W. Jung, H. J. Lee, and Y. S. Lim, "Design of trapezoidal monopole antenna with band notched performance for UWB," *Electron. Lett.*, Vol. 48, No. 12, 673–674, 2012.
7. Kelly, J. R., P. S. Hall, and G. Peter, "Band-notched UWB antenna incorporating a microstrip open-loop resonator," *IEEE Trans. Antennas Propag.*, Vol. 59, Vol. 8, 3045–3048, 2011.
8. Yadav, A., et al., "Slot loaded UWB antenna: Dual band notched characteristics," *Int. J. Electron. Commun. (AEÜ)*, Vol. 70, 331–335, 2016, http://dx.doi.org/10.1016/j.aeue.2015.12.014.
9. Pandey, G. K., H. S. Singh, P. K. Bharti, and M. K. Meshram, "Design and analysis of Ψ-shaped antenna with dual band notched characteristics," *Wireless Pers. Commun.*, Vol. 89, No. 1, 79–92, 2016.
10. Lin, Y., J. Liang, G. Wu, Z. Xu, and X. Niu, "A novel UWB antenna with dual band notched characteristics," *Frequenz*, Vol. 69, Nos. 11–12, 479–483, 2015, http://dx.doi.org/10.1515/freq-2015-0002.
11. Sarkar, D., K. V. Srivastava, and K. Saurav, "A compact microstrip-fed triple band-notched UWB monopole antenna," *IEEE Antennas Wirel. Propag. Lett.*, Vol. 13, 396–399, 2014.
12. Srivastava, G., S. Dwari, and B. K. Kanaujia, "A compact triple band notch circular ring antenna for UWB application," *Microw. Opt. Technol. Lett.*, Vol. 53, No. 3, 668–672, 2015.
13. Kim, D. O. and C. Y. Kim, "CPW-fed ultra-wideband antenna with triple-band notch function," *Electron. Lett.*, Vol. 46, No. 18, 1246–1248, 2010.
14. Wang, Z., J. Liu, and Y. Yin, "Triple band-notched UWB antenna using novel asymmetrical resonators," *Int. J. Electron. Commun. (AEÜ)*, Vol. 70, No. 12, 1630–1636, 2016.
15. Yadav, A., et al., "SRR and S-shape slot loaded triple band notched UWB antenna," *Int. J. Electron. Commun. (AEÜ)*, Vol. 79, 192–198, 2017, http://dx.doi.org/10.1016/j.aeue.2017.06.003.
16. Chu, Q.-X. and Y.-Y. Yang, "A compact ultra-wide band antenna with 3.4/5.5 GHz dual band-notched characteristics," *IEEE Trans. Antennas Propag.*, Vol. 56, No. 12, December 2008.
17. Jyotshna, J. and Sharm, "SRR loaded dual band notched ultra wideband microstrip antenna," *International Journal of Recent Research and Review*, Vol. VII, September 2015.